

Cooperative Fluctuations and Subunit Communication in Tryptophan Synthase[†]Ivet Bahar^{‡,§} and Robert L. Jernigan^{*,‡}

Molecular Structure Section, Laboratory of Experimental and Computational Biology, Division of Basic Sciences, National Cancer Institute, National Institutes of Health, Bethesda, Maryland 20892-5677, and Chemical Engineering Department & Polymer Research Center, Bogazici University, and TUBITAK Advanced Polymeric Materials Research Center, Bebek 80815, Istanbul, Turkey

Received November 11, 1998; Revised Manuscript Received February 1, 1999

ABSTRACT: Tryptophan synthase (TRPS), with linearly arrayed subunits $\alpha\beta\beta\alpha$, catalyzes the last two reactions in the biosynthesis of L-tryptophan. The two reactions take place in the respective α - and β -subunits of the enzyme, and the intermediate product, indole, is transferred from the α - to the β -site through a 25 Å long hydrophobic tunnel. The occurrence of a unique ligand-mediated long-range cooperativity for substrate channeling, and a quest to understand the mechanism of allosteric control and coordination in metabolic cycles, have motivated many experimental studies on the structure and catalytic activity of the TRPS $\alpha_2\beta_2$ complex and its mutants. The dynamics of these complexes are analyzed here using a simple but rigorous theoretical approach, the Gaussian network model. Both wild-type and mutant structures, in the unliganded and various liganded forms, are considered. The substrate binding site in the β -subunit is found to be closely coupled to a group of hinge residues ($\beta 77$ – $\beta 89$ and $\beta 376$ – $\beta 379$) near the β – β interface. These residues simultaneously control the anticorrelated motion of the two β -subunits, and the opening or closing of the hydrophobic tunnel. The latter process is achieved by the large amplitude fluctuations of the so-called COMM domain in the same subunit. Intersubunit communications are strengthened in the presence of external aldimines bound to the β -site. The motions of the COMM core residues are coordinated with those of the α – β hinge residues $\beta 174$ – $\beta 179$ on the interfacial helix $\beta H6$ at the entrance of the hydrophobic tunnel. And the motions of $\beta H6$ are coupled, via helix $\beta H1$ and $\alpha L6$, to those of the loop $\alpha L2$ that includes the α -subunit catalytically active residue Asp60. Overall, our analysis sheds light on the molecular machinery underlying subunit communication, and identifies the residues playing a key role in the cooperative transmission of conformational motions across the two reaction sites.

The tryptophan synthase (TRPS)¹ $\alpha_2\beta_2$ complex is a bifunctional enzyme that catalyzes the last two reactions in the biosynthesis of L-tryptophan (L-Trp). The bacterial enzyme structure consists of two α - and two β -subunits arranged in an extended $\alpha\beta\beta\alpha$ order (Figure 1a,b). The α - and β -subunits contain the respective sites for the α - and β -reactions producing L-Trp: the cleavage of indole 3-glycerol phosphate (IGP) to release indole and glyceraldehyde 3-phosphate (G3P) (α -reaction) and the conversion of indole to L-Trp via a condensation reaction with L-serine (β -reaction). The latter is mediated by the cofactor pyridoxal 5'-phosphate (PLP), which forms with L-Ser a quasi-stable α -aminoacrylate intermediate, E(A–A), highly reactive toward indole. The $\alpha\beta$ -reaction resulting from the combination of



presents a typical example of long-range allosteric effect in that the two reactions, occurring at two topologically distinct

and distant sites, are highly coordinated through a PLP-dependent activation–deactivation mechanism, and the metabolite, indole, is transferred from the active site in the α -subunit to the other in the β -subunit, through a 25 Å long hydrophobic tunnel (Figure 1c,d).

In view of the occurrence of a unique ligand-mediated long-range cooperativity for substrate channeling between two distant reaction sites, and the more general interest of gaining an understanding of the mechanism of allosteric control and coordination in metabolic cycles, the structure and catalytic activity of the bacterial TRPS $\alpha_2\beta_2$ complex (EC 4.2.1.20) and its mutants have been extensively studied. Various methods have been used to this aim, including X-ray crystallography (1–7), site-directed mutagenesis (8–12), and kinetic analyses (10, 11, 13–17). For knowledgeable, informed descriptions of previous work, see the reviews of Miles and collaborators (3, 18–20), and Dunn and co-workers (21).

Crystallographic data provide information about the static characteristics, or equilibrium properties, in general. Yet, indirect information about the conformational flexibility of

[†] This work was supported by NATO CRG 951240 and the Intramural NCI Program.

[‡] National Institutes of Health.

[§] Bogazici University and TUBITAK Advanced Polymeric Materials Research Center.

¹ Abbreviations: TRPS, tryptophan synthase; GNM, Gaussian network model; IGP, indole 3-glycerol phosphate; G3P, glyceraldehyde 3-phosphate; PLP, pyridoxal 5'-phosphate; IPL, indole 3-propanol phosphate; E, Schiff base; E–Ser, serine pyridoxal 5'-phosphate Schiff base; E–Trp, L-tryptophan pyridoxal 5'-phosphate Schiff base.

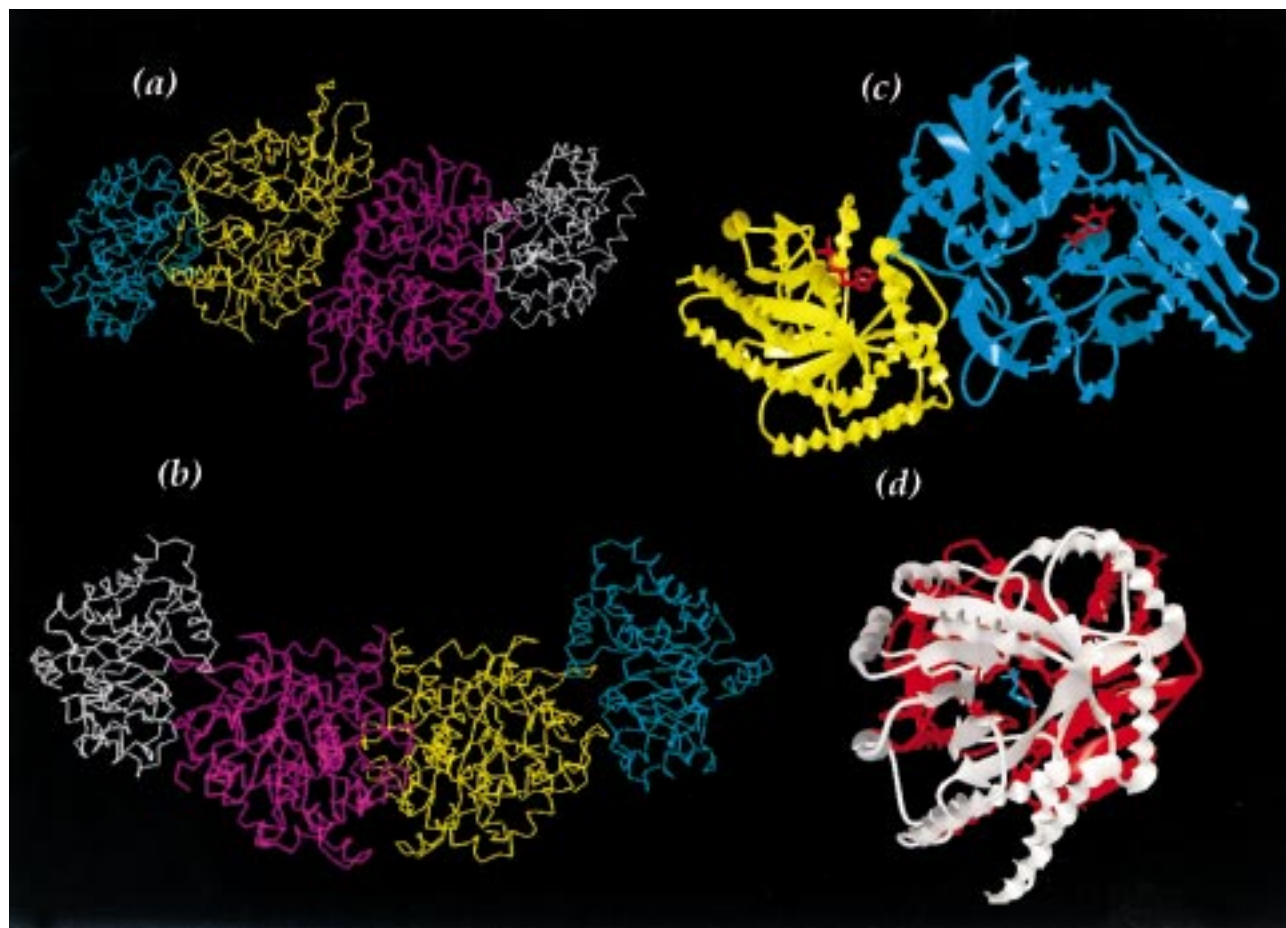


FIGURE 1: Schematic representations of the overall fold of the TRPS $\alpha_2\beta_2$ tetramer and ribbon diagrams of the $\alpha\beta$ dimeric part with the bound ligands. Panels a and b depict the tetramer from two different viewpoints. The α -subunits are blue and white, and the β -subunits are yellow and magenta. The tunnel for indole channeling can be distinguished between the N- and C-terminal domains of β -subunits (a). Panel c is the ribbon diagram of the dimeric portion $\alpha\beta$ based on a mutant α D60N (PDB file 1a5b; see Table 1), having the α -reaction substrate IGP (red) bound to the active site of the α -subunit (yellow), and the β -reaction cofactor PLP (red) covalently bonded to the β -subunit (blue). An alternative ribbon diagram of the dimer is shown in panel d, based on the wt structure 1wsy, with the α -subunit depicted in white and the β -subunit in red. Panels c and d provide two different views of the tunnel for indole channeling between the α - and β -active sites.

the TRPS complex could be approached from X-ray studies by examining the changes in residue coordinates in the presence of different substrates or cations (4, 5). Certain residues in the β -subunit were found for example to be displaced as much as 5 Å in liganded mutants (β K87T), compared to their positions in the unliganded wild-type structure (5). Another dynamic feature emerging from both the X-ray crystallographic and other kinetic studies is the high mobility of certain loops (α L2 and α L6) in the α -subunit, whose conformational motions might be directly relevant to intersubunit communication. Overall, these studies contributed to an assessment of the role of the hydrophobic tunnel in directing the diffusion of indole between the α - and β -reaction sites and conveying the allosteric signals that synchronize the two reactions. These signals are proposed to trigger a conformational change from an open (low activity) to a closed (high activity) state upon formation of the E(A-A) intermediate, which prevents the escape of indole (7, 21).

As pointed out in a recent review by Dunn and collaborators, “for efficient substrate channeling, a rather stringent set of physical and dynamic constraints must be met”, and “the architecture of the multienzyme complex must provide a physical structure with dynamic properties that constrain the degrees of freedom of the metabolite” (21). A direct

Table 1: Structures Investigated in This Study

PDB file	structure	resolution (Å)	substrate/ligand	ref
1wsy	wt $\alpha_2\beta_2$	2.5	E, Na ⁺	2
1bks ^a	wt $\alpha_2\beta_2$	2.2	E, Na ⁺	private communication
1ttq	wt $\alpha_2\beta_2$	2.0	E, K ⁺	4
2tys	β K87T $\alpha_2\beta_2$	1.9	E-Trp, Na ⁺	5
1a5b	α D60N $\alpha_2\beta_2$	2.0	E, IGP, K ⁺	6
2trs	β K87T $\alpha_2\beta_2$	2.04	E-Ser, IPL, Na ⁺	5

^a Theoretical results for the wild-type TRPS will be based on the more refined structure 1bks recently determined by Hyde and collaborators.

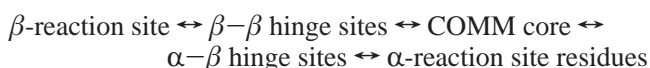
analysis of the dynamic characteristics of TRPS $\alpha_2\beta_2$ complexes (Table 1) is undertaken in this study for elucidating details of the molecular machinery which controls the coupling between the different subunits. Both wild-type and mutant structures, in the unliganded and in various liganded forms, will be considered.

Our theoretical approach, the so-called Gaussian network model (GNM) of proteins, uses known crystal coordinates, or more exactly the known topology of protein-protein or protein-ligand contacts at the level of individual residues, to determine the dominant modes of motions for the

particular architecture (22–25). Correlated movements with different length scales, which may bear direct relevance to biological function, are identified on the basis of the premise of structure-defined function. Recent applications of the GNM to a number of biomolecular systems, including the tRNA–synthetase complex (26), HIV-1 reverse transcriptase (27), HIV-1 protease (25), and several monomeric proteins such as apomyoglobin (23), cytochrome *c*, chymotrypsin inhibitor 2, and CheY (28), have proven its utility for disclosing the dynamic features imparted by the intricate three-dimensional networks of contacts of different folded structures.

In the GNM analysis of TRPS complexes, the following issues will be considered. Which residues assume a functional role in the specific three-dimensional structure of the complex? In particular, which residues act as hinges in the global motions, and which conversely enjoy a relatively high degree of conformational freedom? Residues in the former group typically participate in substrate binding and catalysis, and their mutation might cause functional impairment; residues in the latter group are typically involved in substrate recognition. Their deletion or substitution might affect the catalytic activity in more indirect ways, such as the less efficient recognition of substrate, or even blocking access to the active site. Changes in the dynamics of the enzyme caused by the absence or presence of substrates will be pointed out. Results will be discussed with regard to existing experimental data about the structure and catalytic activity of TRPS complexes.

Finally, a mechanism for driving the allosteric effects across the tetramer, via the β – β and α – β intersubunit interfaces, will be proposed here, based on observed cross-correlations between motions of different structural elements. Essentially, the structural elements facilitating the communication and their linking between the α - and β -reaction sites will emerge as



(see Table 2). The β – β and α – β hinge residues assume a key role in this global processing, irrespective of ligand binding, whereas the cooperativity of the COMM core is enhanced only in the presence of PLP derivatives at the β -site.

MATERIALS AND METHODS

Structures. The crystal structures analyzed in this study are listed in Table 1. The wild-type (wt) structure of the TRPS $\alpha_2\beta_2$ complex from *Salmonella typhimurium* [Brookhaven Protein Data Bank (PDB) file 1wsy] was determined a decade ago by Hyde et al. (2), and recently refined (1bks) by the same group to 2.2 Å resolution (C. C. Hyde et al., personal communication). In these structures, the coenzyme PLP forms a Schiff base (E) with the ϵ -amino group of β Lys87. Additionally, the wt structure (1ttq) having K⁺ (instead of Na⁺) bound to the C-terminal domain of the β -subunit will be analyzed. The recently determined higher-resolution wt structure (1bks) will be taken as representative of the intrinsic dynamics of the multienzyme in the absence of substrate. Its behavior will be contrasted to those of the

Table 2: Critical Structural Elements of Interest Emerging from GNM Analysis of the Dominant Modes of Motion of TRPS Complexes^a

structural element ^b	residues	peak locations	secondary structure at peak position	dynamic function
α-Subunit				
1 (23)	9–16	Arg14	α H0' C-terminus	highly flexible
2 (24)	35–44	Ala43	α H1 C-terminus	highly flexible
3 (25)	192–196	His194	α H6 N-terminus	highly flexible
4 (26)	216–225	Ala222	α H7	highly flexible
5 (27)	246–268	Ala253, Lys249	α H8	highly flexible
6 (28)	54–60	Leu58, Ala59	α L2	α – β hinge
7 (29)	102–110	Asn104	α L3	α – β hinge
8 (30)	129–136	Asp130, Pro132	α L4	α – β hinge
9 (31)	179–183 ^c	Gly181	α L6	α – β hinge
β-Subunit				
10 (32)	288–295	Asp291	β L8	α – β hinge
11	14–24	Pro18, Gln19	β H1 N-terminus	α – β hinge
11' (33)	18–44	Glu40, Gln36	β H1– β H2	α – β hinge
12 (34)	174–179 ^c	Arg175	β H6	α – β hinge
13 (35)	277–283	Ile278, Tyr279	β L8	α – β hinge
14 (36)	48–67	Asn51, Thr57	β H2, β S1	β – β hinge
15	79–82	Leu80	β L2	β – β hinge
15' (37)	77–89	Leu80, Gly84	β L2	β – β hinge
16 (38)	337–346	Cys340, Gly344	β H11	β – β hinge
17 (39)	376–379	Ser377, Gly378	β L10	β – β hinge
18 (40)	130–145	Lys137, Ala136	β L4, β H5	COMM core
19 (41)	155–170	His160, Gly162	β L5	COMM core
20 (42)	383–393	Asp393	β H13 C-terminus	highly flexible
21 (43)	221–233		β S7	highly flexible

^a Regions 1–16 were identified from the first (slowest) principal mode of motion. The corresponding highly flexible residues are green in Figure 4, those identified as hinges at the α – β interface red (α -subunit) or pink (β -subunit), and the β – β hinge residues magenta. Regions 11', 15', and 17–21 appear following analysis of the 10 dominant modes. ^b The numbers in parentheses represent the serial indices for the structural elements in subunits α_2 and β_2 . ^c Calculated for the complex (2trs) having substrates bound on both α - and β -sites (5).

ligand-bound enzymes or mutants. Toward this aim, a series of mutants will be considered.

First, mutants having ligands bound to either α - or β -sites will be considered. Examples are the mutant β K87T $\alpha_2\beta_2$ complex with the L-Trp bound as an external aldimine (E–Trp) with PLP at the active site of the β -subunit (2tys) and mutant α D60N with the true substrate (IGP) at the α -subunit (1a5b). E–Trp is the kinetic intermediate preceding the release of L-Trp. This is the protonated form of the quinonoid intermediate (E–Q), a substance resulting from the nucleophilic attack on E(A–A) by indole. Second, a complex with ligands bound to both α - and β -sites will be considered (2trs). Therein, L-Ser is bound to the β -subunit active site, as an external aldimine (E–Ser) with PLP, and the substrate analogue indole 3-propanol phosphate (IPL) is bound to the α -subunit active site. See Table 1.

The α -subunit has an eight- α/β barrel fold closely related to the structure of triose phosphate isomerase (TIM) barrels, whereas the fold of the β -subunit is unique. In this paper, we adopt a nomenclature commonly used (2, 7) for referring to the secondary structural elements of the respective subunits. Accordingly, the α/β barrel helices and strands of the α -subunit are designated as α H1– α H8, and α S1– α S8, respectively; there are three extra helices in the α -subunit, α H0, α H2', and α H8' indexed in conformity with their sequential positions. The β -subunit, on the other hand, has two topologically similar domains (2), overall including

helices $\beta\text{H1}-\beta\text{H13}$ and strands $\beta\text{S1}-\beta\text{S10}$. For brevity, the notation αLi (or βLi) will be adopted for the loop immediately succeeding the strand αSi (or βSi). The subunits themselves will be referred to as α_1 , β_1 , β_2 , and α_2 .

Theoretical Model and Method. The method (22, 23) relies on modeling the protein structure as a network of contacts between all α -carbons separated by a distance r of ≤ 7 Å. This interaction range includes neighbors within a first coordination shell in the vicinity of a central residue. It automatically includes the first and second neighbors along the chain sequence, and therefore takes into account chain connectivity. But more importantly, the intricate topology of contacts between all nonbonded pairs in the folded state is taken into consideration. The latter play a dominant role in defining the overall molecular machinery. The interactions are assumed to obey a harmonic form. Therefore, the α -carbons undergo Gaussian fluctuations near their equilibrium positions, hence the name Gaussian network model (GNM). No distinction between different types of side chains is made here, except that implicit in the details of the structure. Thereby, a mechanistic description, purely entropic in origin, is adopted.

The topology of contacts is accounted for by a Kirchhoff matrix of contacts Γ in the GNM. For a three-dimensional structure of n sites (residues, nucleotides, and/or ligand functional groups), this is an $n \times n$ symmetric matrix whose ij th off-diagonal element is assigned a value of -1 or 0 , depending on the presence or absence of a contact, respectively, between sites i and j . As such, Γ contains the same information as do customary contact maps. As for the i th diagonal element of Γ , it is evaluated as the negative sum of all elements in the i th row (or column). It is thus equal to the coordination number of site i . Therefore, Γ contains two basic kinds of structural data: the local packing density in the neighborhood of each site (diagonal elements) and the order of contacts, as described by the sequence index $1 \leq i \leq n$ of interacting sites, i.e., the non-zero off-diagonal elements.

From statistical mechanics, Γ is the matrix of force constants maintaining the overall structure in a stable form near its folded state, inasmuch as the internal Hamiltonian of the structure may be written as (25)

$$H = \frac{1}{2} \gamma [\Delta \mathbf{R}^T (\Gamma \otimes \mathbf{E}) \Delta \mathbf{R}] \quad (1)$$

where γ is a single parameter (Hookean force constant) that uniformly scales the strengths of all pairwise interactions, $\Delta \mathbf{R}$ is the $3n$ -dimensional vector of the x -, y -, and z -components of the fluctuations $\Delta \mathbf{R}_1, \Delta \mathbf{R}_2, \dots, \Delta \mathbf{R}_n$ in the positions of the n sites, the superscript T denotes the transpose, \otimes is the direct product, and \mathbf{E} is the identity matrix of order 3. In parallel with classical normal mode analyses, the inverse of Γ yields information about the auto- or cross-correlations between the motions of individual residues, following the relationship

$$\langle \Delta \mathbf{R}_i \cdot \Delta \mathbf{R}_j \rangle = (3kT/\gamma) [\Gamma^{-1}]_{ij} \quad (2)$$

where k is the Boltzmann constant, T is the absolute temperature, and $[\Gamma^{-1}]_{ij}$ designates the ij th element of the inverse of Γ . For more details, the reader is referred to our recent studies (22, 25), or to the original statistical thermo-

dynamic theory of Gaussian networks (29, 47). The suitability of a single parameter γ for the force constant of all contacting residue pairs was first demonstrated by Tirion (30).

Information about global dynamics is acquired by decomposing the motions into a series of modes, and concentrating on the modes at the slowest end of the spectrum which contribute the most to the total range of motions. This modal decomposition is performed in the GNM, by an eigenvalue transformation of Γ (23, 26, 30) which yields a total of $n - 1$ modes of motion differing in their frequencies (eigenvalues) by about 3 orders of magnitude for a system of 10^3 sites. We note that in tetrameric form, the TRPS complex comprises about 1300 sites, and therefore ~ 1300 modes. Yet, only a small subset (~ 10) of the slowest modes dominate the global motions. The slowest mode is referred to as the first principal mode of motion or the global motion.

The correlation $[\Delta \mathbf{R}_i \cdot \Delta \mathbf{R}_j]_k$ contributed by the k th mode is found from

$$[\Delta \mathbf{R}_i \cdot \Delta \mathbf{R}_j]_k = (3kT/\gamma) [\lambda_k^{-1} \mathbf{u}_k \mathbf{u}_k^T]_{ij} \quad (3)$$

where \mathbf{u}_k is the k th eigenvector of Γ and λ_k is the k th eigenvalue. The correlations that operate in a subset of modes of interest ($k_1 \leq k \leq k_2$) are evaluated by weighting the contribution of each mode by $1/\lambda_k$.

In this paper, we will concentrate on the first principal mode, and on a representative subset of modes at the dominant (slow) end of the spectrum. The statistical weight ω_2 of the first principal mode amounts to approximately $1/5$ of the entire spectrum in the present complexes, as estimated from the ratio $\omega_2 = (1/\lambda_2)/\sum_i 1/\lambda_i$ ($2 \leq i \leq n$). This mode reflects the most cooperative mechanism of action of the overall quaternary structure. It will be shown to be uniquely defined for TRPS tetramers, in general. The subset of 10 slowest modes, on the other hand, is found to add up to more than half of the spectrum. This subset will be shown to differentiate among the motions undergone by the different TRPS complexes, as described below.

RESULTS

Comparison with X-ray Crystallographic B Factors. Our objective is to assess the dominant modes of motion that operate in the transmission of allosteric effects in the TRPS $\alpha_2\beta_2$ complex. Rather than the thermal fluctuations of individual residues, the cooperative motions propagated over the distance scale of the excursion of the substrates in the overall complex are of interest. Within this scope, the slowest (and largest amplitude) motions undergone synchronously by different structural elements will be examined, along with the effect of substrate binding on the dominant mechanism of motion. However, before proceeding to a detailed analysis of the dominant modes of motion, we have first tested the accuracy and applicability of the GNM as specifically applied to TRPS complexes (Table 1) by comparing the mean-square (ms) fluctuations of residues predicted by the GNM with those indicated by X-ray crystallography.

The X-ray crystallographic B factors, also referred to as the Debye-Waller or temperature factors, provide a measure of the fluctuations of individual residues in folded structures. Neglecting crystal imperfections and/or static disorder effects, they are related directly to our calculated mean-square (ms)

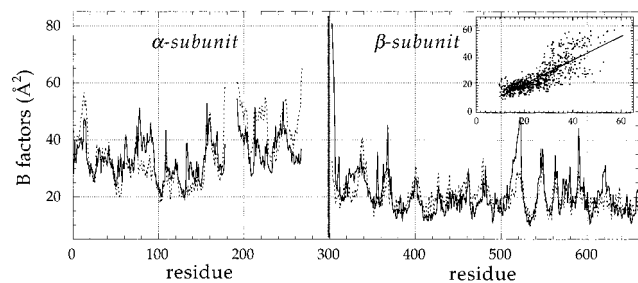


FIGURE 2: Comparison of the theoretical (solid curve) and experimental (small dashed curve) temperature factors for α -carbons in the mutant β K87T $\alpha_2\beta_2$ tetramer. Results for only subunits α_1 and β_1 are displayed; those for subunits α_2 and β_2 are identical. Experimental data were taken from PDB file 2tys deposited by Rhee et al. (5). Theoretical results were calculated using eqs 2 and 4. Discontinuities in the curves correspond to the structural regions that are invisible in X-ray experiments. The inset displays the theoretical results plotted against the experimental ones. The correlation coefficient between the two sets of data is 0.80.

fluctuations by

$$B_i = (8\pi^2/3)\langle \Delta \mathbf{R}_i \cdot \Delta \mathbf{R}_i \rangle \quad (4)$$

which permits a direct comparison between theory and experiments. Here the angular brackets refer to the average over all modes of motion.

Results for a relatively high-resolution structure, 2tys (Table 1), are illustrated in Figure 2. Experimental results (small dashed) are taken directly from the PDB file (5). The theoretical (solid) curve is calculated using eqs 2 and 4. The constant γ , which scales overall the theoretical curve to match the experimental data reported (5) for this protein, is taken here as $0.46 \text{ kcal mol}^{-1} \text{ \AA}^{-2}$. The discontinuity at α -subunit residues 178–191 corresponds to loop α L6 which was reported not to be visible in the crystal structure. In the inset, the theoretical B factors are plotted against the experimental ones. The correlation coefficient between the two sets of data is found to be 0.80. This level of agreement is quite satisfactory in view of the simplicity of the model. The agreement is better than that obtained with atomic scale molecular dynamics simulations in which multiple minima are visited, because the space accessible to vibrational motions near the folded state, which essentially determines the crystallographic B factors, is rigorously treated in the GNM analysis. In the case of MD simulations, we note that shorter simulations, limited to fluctuations near the folded state, give better agreement with experimental B factors than longer simulations.

Calculations for the other structures led to theoretical curves similar to the example depicted in Figure 2. GNM results are relatively insensitive to small shifts in atomic coordinates. However, the correlation between theory and experiment slightly diminishes with a decrease in the quality of the resolution of the crystal structure. In the case of the two wt structures, for example, the experimental B factors for the more refined structure were more consistent with the theoretical results, which lends further support to the utility and applicability of the GNM.

Global Motion Driven by the First Principal Mode of Action. Figure 3 illustrates the ms amplitudes of motion of the individual residues, under the action of the first principal mode (slowest one). Parts a and b refer to subunits α and β ,

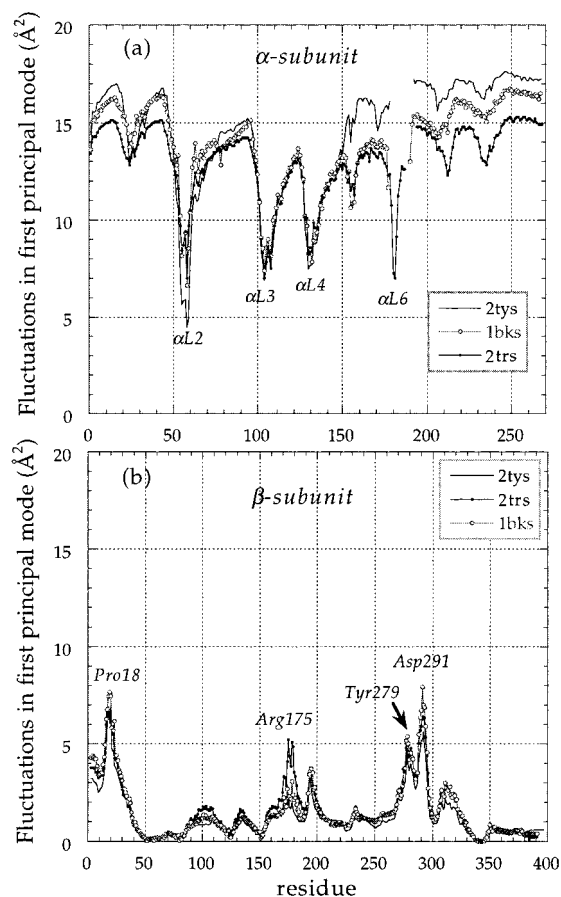


FIGURE 3: Mean-square (ms) amplitudes of residue fluctuations driven by the first principal mode of motion representative of the cooperative movements on a global scale. Results are displayed for the wt structure 1bks, and for two mutants, 2tys and 2trs. See Table 1. Panels a and b describe the behavior of the α - and β -subunits, respectively. Note the significant difference in the amplitudes of motions of the two subunits. The three curves exhibit similar features, in general. This reveals the unique dependence of the global dynamics on the particular tetrameric architecture, irrespective of the shifts in coordinates caused by substrate binding. See Figure 4 for the spatial position of peaks and minima and Table 2 for their identities and secondary structures. The maxima in panel a are the most flexible regions of the enzyme. The minima therein form the α - β hinge sites, together with the maxima in panel b which exhibit comparable amplitudes of fluctuation. Finally, the minima in panel b are the β - β hinge sites in the global mode of motion.

respectively. Results are shown for the refined wt structure (1bks), and for two mutants (2tys and 2trs) having one and two bound substrates, respectively (Table 1). Results for the K^+ -bound (1ttq) and the IGP-bound (1a5b) structure obey the same trend; these are not shown for visual simplicity.

The first principal mode of motion of the different TRPS complexes is found to be uniquely defined, irrespective of the presence or absence of substrates. In fact, this mode may be viewed as representative of the fundamental mechanical behavior of the structure on a gross scale. It defines the most probable mechanism of action. And this should be, in principle, a unique function of the particular enzyme, i.e., a signature of its overall molecular architecture. Substrates will be shown below to affect more the immediate next higher frequency modes. The latter are still long-range in nature, but slightly more localized.

We now proceed to examine the shape of the first principal mode. The first observation is the significantly higher

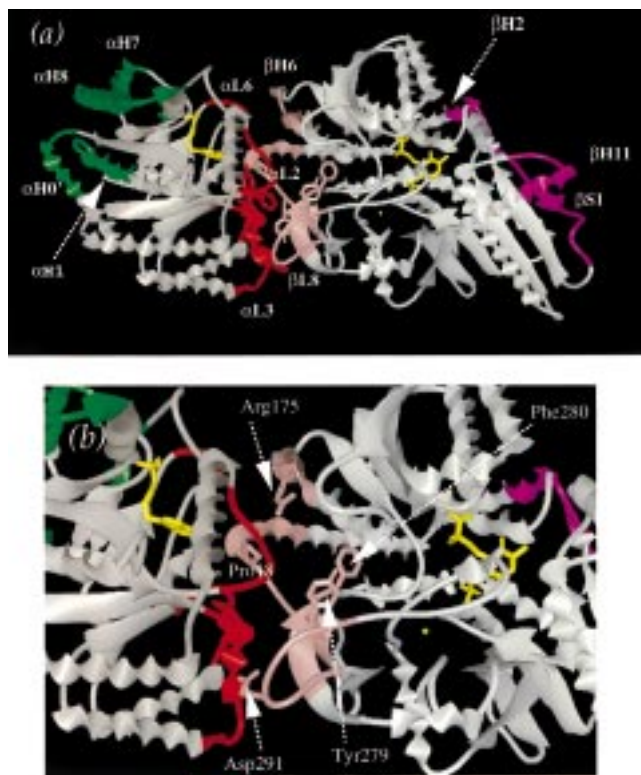


FIGURE 4: (a) Schematic representation of TRPS regions distinguished by (i) their high flexibility (maxima in Figure 3a, green), (ii) their action as hinges for the movement of the α -subunit relative to the β -subunit (minima in Figure 3a, red), (iii) their involvement in the α - β intersubunit coupled motions, evidenced by their fluctuation amplitudes matching those observed in the α -subunit hinge residues (maxima in Figure 3b, pink), and (iv) their rigidity (minima in Figure 3b, magenta), in the global motion of the tetramer. The corresponding residue (sequential) numbers and peak positions are listed in Table 2. The diagram is drawn using the PDB coordinates (2trs) of a mutant (β K87T) having two substrates, IPL on the α -site and E-Ser on the β -site. The substrates and the β -subunit cation Na^+ are yellow. A few aromatic residues implicated in the α - β hinge motion are explicitly shown. We distinguish in particular β Tyr279 and β Phe280 acting as a molecular gate for the tunnel, and α Phe54 and α Tyr102 at a central position among the α -subunit hinge residues. (b) A closer view of the α - β interface region. The β -subunit residues at the peak positions of Figure 3b are explicitly shown.

mobility of the α -subunit, compared to that of the β -subunit. The ms amplitudes of motions undergone in the α -subunit are larger than those in the β -subunit by about 1 order of magnitude.

The horizontal lines in Figure 3a divide the residues into three groups with different flexibilities, approximately. The uppermost part refers to the most flexible regions, shown in green in Figure 4. See Table 2 (first five rows) for the sequential position and secondary structure of these residues. The lowermost region, on the other hand, comprises residues acting as hinges, or anchors, for the global motion of the α -subunit. These are shown in red in Figure 4 and are clustered together at the α - α intersubunit interface, despite the fact that they belong to four sequentially discontinuous stretches (Table 2, rows 6–9). Their location suggests that they are active in modulating the global motion of the α -subunit relative to the β -subunit, hence the name α - β hinge residues adopted here for designating these residues. Coupled to them are a small group of residues in the β -subunit, which exhibit about the same magnitudes of

motion (maxima in Figure 3b). These, shown in pink in Figure 4, undergo in-phase cooperative motions with the hinge residues of the α -subunit, as indicated by interresidue cross-correlations (see below). Several aromatic residues (α Phe54, α Tyr102, α Phe107, α Pro132, β Tyr16, β Pro18, β Tyr279, and β Phe280) are found to participate in this α - β hinge region. A closer view of the interface is presented in part b of Figure 4, which displays the β -subunit residues distinguished by their unique behavior at the center of α - β hinge sites.

Finally, of interest is the group of residues most completely hindered in the global motion of the tetramer. These lie at the minima of the curve in Figure 3b. Residues located at the interface between the two β -subunits, near the β -subunits' substrate binding site, are found to form this group. These will be shortly referred to as the β - β hinge residues. It is conceivable that these severely constrained residues play a critical role in controlling the stability and/or flexibility of the β_2 dimer, which is known to be stable and active as a dimer in the absence of the α -subunit (18, 20). Their location near the β -subunit active site also suggests their involvement in mediating the conformational changes associated with the β -reaction catalysis. The analysis of auto- and cross-correlations driven by a dominant subset of modes, presented below, will in fact reveal the critical role of these residues in monitoring the communication across subunits. A summary of the regions of interest presently mentioned is given in Table 2, along with the positions of the corresponding peaks and minima. The latter will be referred to as the critical locations emerging in the first principal mode of motion.

Effect of a Representative Subset of Dominant Modes. The first principal mode of motion has been seen above to be insensitive to bound ligands. The effects of different bound ligands will however be distinguishable upon examination of the cumulative effect of a subset of dominant modes. We consider here the combined effect of 10 slowest modes. This subset incorporates the majority of operative modes, from a statistical point of view, while excluding relatively more localized or random motions that might obscure our understanding of the overall molecular machinery.

Results are presented in Figure 5. Parts a and b refer to the α - and β -subunits, respectively, similar to Figure 3. Results for the refined wt structure (1bks) and two mutants (2tys and 2trs) are displayed (Table 2).

The behavior of the α -subunit (Figure 5a) is rather similar to that revealed in the first principal mode (Figure 3a). The main differences that arise from the contribution of the newly included modes are as follows. Among the three peaks observed at the C-terminal segment in Figure 3a, two survive, and are even further enhanced (α L6 N-terminus and α H8; see Table 2). The peak near helix α H5 becomes more pronounced, in particular in the E-Trp-bound form, so this is direct evidence of the effect binding in the β -subunit has on the motions of the α -subunit. These three most mobile regions are green in Figure 6a, along with the most mobile part of the β -subunit, the C-terminal end, including the N-terminal half of helix β H13.

The α -subunit critical loci at the α - β interface (minima in Figure 5a) remain almost unchanged as one proceeds from the first principal mode to a subset including the immediate higher-frequency modes. See the red regions in part a of Figure 6. The α - β hinge residues on the β -subunit exhibit,

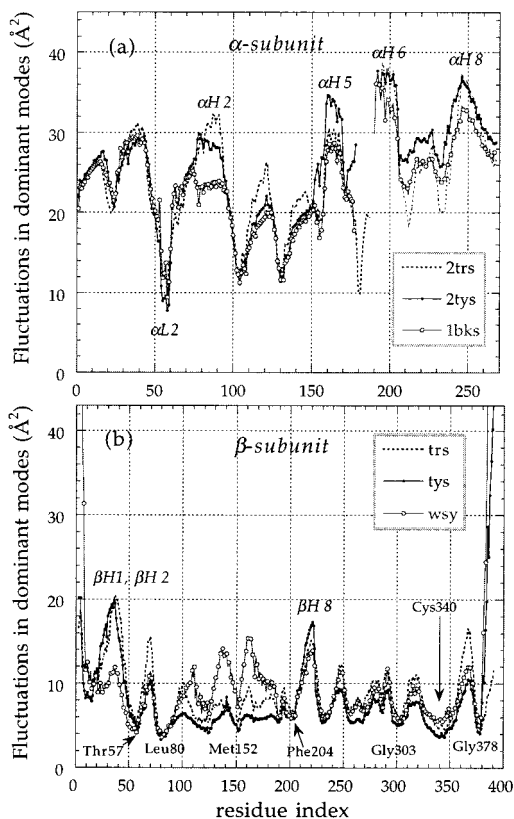


FIGURE 5: Distribution of ms fluctuations in the dominant modes of motion, shown for three structures, the wt 1bks and two mutants, 2tys having a β -subunit substrate bound and 2trs with substrate bound to both α - and β -subunits (Table 1). Panels a and b depict data for the α - and β -subunits, respectively. See Figure 6a and its legend for the location of (i) the most flexible regions (green), (ii) the minima in panel a and the maxima in panel b participating in the α - β hinge sites, and (iii) the most severely constrained regions of the overall tetramer at the lowest minima of panel b (magenta). Note the increase in the mobility of $\alpha H2$ and $\alpha H5$ in the presence of β -site substrates. Minima in panel b refer to residues subject to highly restrictive dynamics in the global motion of the tetramer, some of which are denoted by the labels. A closer examination showed that the sequence LLHGG of residues $\beta 80$ – $\beta 84$ forms the lowest minimum in all complexes.

however, more variation. Helices $\beta H1$, $\beta H2$, and $\beta H8$ are distinguished here by their large amplitudes of motion, comparable to those of the α -subunit α - β hinge residues. These latter regions ($\beta 18$ – $\beta 44$ and $\beta 211$ – $\beta 223$) are also shown in red in the same figure.

Finally, the loci of the β - β interface hinges (magenta) are slightly shifted in general. We note the addition of $\beta L10$ residues $\beta 376$ – $\beta 379$ to this group, and the broadening of the hinge region centered around β Leu80. The latter now covers residues $\beta 77$ – $\beta 89$. In all of the five examined structures, this region was found to yield the deepest minimum (Figure 5b). It is noteworthy that residue β Lys87, to which the cofactor PLP is covalently linked, is also included in this interval. This provides firm evidence that the β -reaction site is directly controlled by the presently investigated set of dominant modes.

Residues $\beta 77$ – $\beta 89$ that act as anchors near the β -reaction site are, at the same time, located at a hinge site between the two topologically similar domains of the β -subunit (Figure 6b). This indicates that these residues are involved in mediating the interdomain separation within the β -sub-

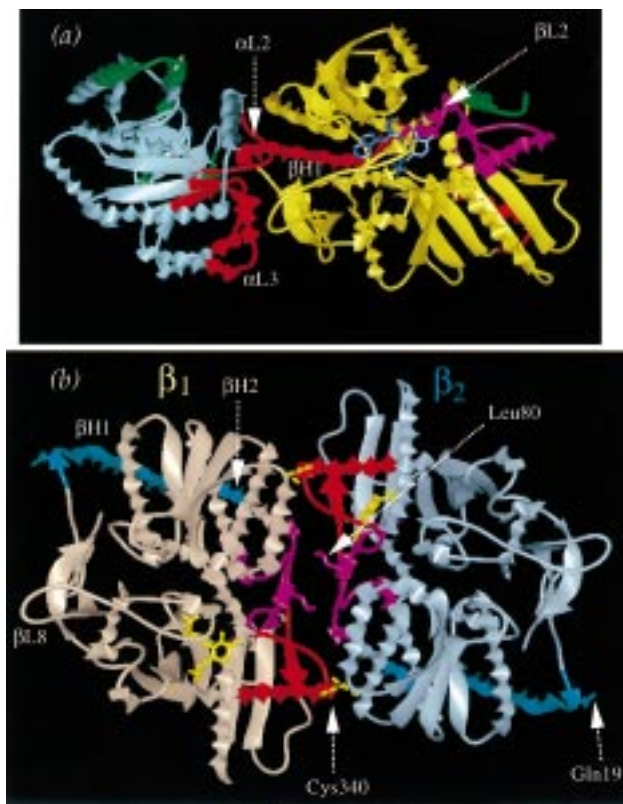


FIGURE 6: (a) Regions with different flexibilities distinguished in the dominant (slowest) modes of motions (Figure 5), shown for the $\alpha_1\beta_1$ dimeric part of 2tys (Table 1). The most constrained regions are magenta. These are all β -subunit residues ($\beta 77$ – $\beta 89$ and $\beta 333$ – $\beta 348$, and $\beta 376$ – $\beta 379$ and $\beta 49$ – $\beta 60$) near the β -reaction site and β - β interface. Shown in red are the most severely constrained residues of the α -subunit ($\alpha 54$ – $\alpha 60$, $\alpha 100$ – $\alpha 114$, and $\alpha 126$ – $\alpha 140$), and those, in the β -subunit, which exhibit similar amplitudes of motion ($\beta 18$ – $\beta 44$ and $\beta 211$ – $\beta 223$). The most mobile regions are green. These are residues $\alpha 192$ – $\alpha 205$, $\alpha 240$ – $\alpha 257$, and $\alpha 159$ – $\alpha 169$ in the α -subunit and $\beta 387$ – $\beta 397$ at the C-terminal end of the β -subunit. See Table 2 for the corresponding secondary structures and critical loci. (b) Ribbon diagram of the β - β dimeric portion. Two different groups of constrained residues are distinguished: (i) those involved in the correlated motion of the N- and C-terminal domains (magenta), also controlling the breadth of the tunnel for indole channeling, and (ii) those monitoring the concerted motion of the two β -subunits (red). The corresponding most constrained residues are Leu80 and Cys340. These two critical loci are denoted in the diagram, along with a few other residues of interest. See Table 2. Note the close interaction (yellow dashed lines) between β - β hinge residues $\beta 333$ – $\beta 348$ and the COMM region (see Figure 8) of the adjacent subunit.

units. More importantly, this mechanism of motion directly modulates the enlargement or restriction of the hydrophobic tunnel located at the cleft between the N- and C-terminal domains of the β -subunits. Thus, the subset of presently identified key residues near the β - β interface comprise two groups: those involved in intersubunit (β - β) communication and those controlling the interdomain spacing within the β -subunits, and thereby the width of the tunnel for indole channeling. The former comprises residues $\beta 333$ – $\beta 348$ and $\beta 60$ – $\beta 62$ and the latter $\beta 77$ – $\beta 89$, $\beta 376$ – $\beta 379$, and $\beta 48$ – $\beta 59$ approximately. These are red and magenta, respectively, in part b of Figure 6. Therein, the β - β dimeric portion of the tetramer is shown. A few residues of interest mentioned above (see also Table 2) are displayed. For clarity, C-terminal residues $\beta 381$ – $\beta 393$ (overlapping with the magenta residues, as observed from this viewpoint) have been removed.

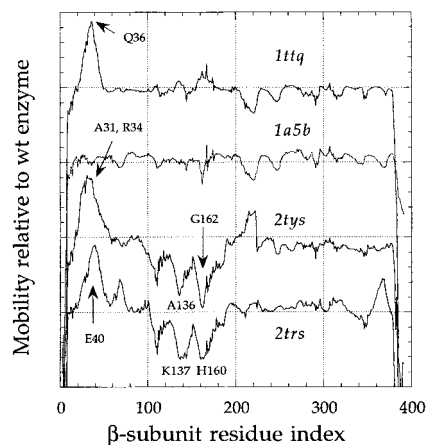


FIGURE 7: Changes in the mobility of β -subunit residues in liganded mutants, compared to that of the wt structure. Results refer to the differences in the ms fluctuations in the four mutants denoted by the labels, relative to that of the wt structure. See Table 1. The most significant changes are (i) an enhancement in the mobility of helix β H1 (and N-terminal half of β H2), mainly residues β 18– β 44, in 1ttq, 2tys, and 2trs, and (ii) a severe hindering of the flexibility of the COMM domain, residues 103–187, in the two structures (2tys and 2trs) with external aldimines bound on the β -site. Some residues at extrema are indicated. See Figure 8.

Changes in Mobilities Induced upon Ligand Binding. Figure 7 provides a direct view of the changes to the mobilities of the different regions of β -subunits in the liganded mutants, compared to the wt structure. Here, we see the differences between the residue fluctuations in the investigated liganded structures (Table 1) and those occurring in the wt case. For clarity, the curves are vertically shifted, and the baseline for each of them is indicated by dotted lines. The uppermost curve displays for example the perturbation in the dynamics of 1ttq, relative to those of 1bks. The most significant change therein is an enhancement in the mobility of helix β H1 and its near neighbors along the sequence (red in Figure 6a and blue in Figure 6b), mainly residues β 18– β 44, with a peak at β Gln36. The same effect is also revealed in 2tys and 2trs, suggesting that the presence of an external aldimine (E–Ser or E–Trp) or a large cation (K^+) bound to the β -subunit enhances the mobility of β H1. We recall that the terminus of β H1 was distinguished in the first principal mode as an α – β hinge site, its motion being closely coupled to that of loop α L2 comprising the catalytically active site. This region is now expanded to embrace the entire helix β H1 and the succeeding loop and helix (α H2). Interestingly, β H1 is a long (18-residue) helix, extending from the α – β interface deeply into the β -subunit (Figure 6a,b), and its high mobility coupled to the α -reaction site may have dynamic implications for its role in transmitting information across the subunits, as also suggested by the cross-correlations examined below.

In contrast to β H1, the region between residues β 103 and β 187 in the N-terminal domain of the β -subunit exhibits a depressed mobility in 2trs and 2tys, the two structures with external aldimines bound on the β -site. Inasmuch as this feature is not observed in any of the other structures, we can interpret it as an effect of β -site substrates on the dynamics of complexes. In Figure 8, we show in pink the region exhibiting this pronounced hindered mobility in the presence of substrates, and in magenta its most strongly affected segments (β 130– β 145 and β 155– β 170). This region (β 103– β 187) closely matches the so-called COMM

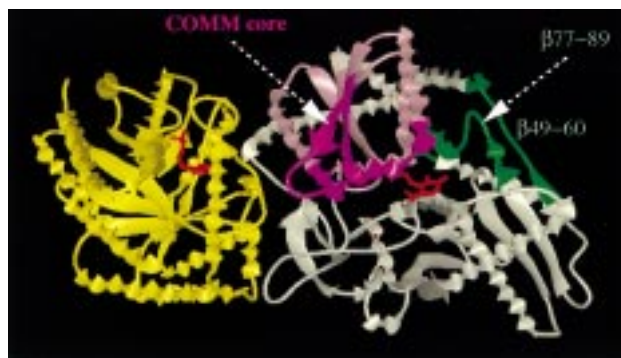


FIGURE 8: Ribbon diagram displaying in pink and magenta the β -subunit COMM domain backbone emerging from Figure 7 as the region undergoing a significantly diminished mobility in the presence of β -site substrates. The most strongly affected segments (β 130– β 145 and β 155– β 170) are magenta. Shown in green are two stretches of residues acting as anchors for the relative motions of the N- and C-domains of the β -subunit. See the legend of Figure 6b.

domain of the β -subunit which was pointed out by Schneider et al. (7), as a slight modification of the “mobile region” originally pointed out by Rhee et al. (5), to play an important role in the allosteric communication between the α - and β -sites. The most severely affected regions identified here (β 130– β 145 and β 155– β 170) will be referred to as the COMM core regions below.

Cross-Correlations between Different Structural Elements. We now focus on the orientational couplings between the motions of different structural elements. To this aim, cross-correlations $\langle \Delta \mathbf{R}_i \cdot \Delta \mathbf{R}_j \rangle$ between the fluctuations of residues i and j ($1 \leq i < j \leq n$) are calculated and normalized as

$$C_{ij} \equiv \langle \Delta \mathbf{R}_i \cdot \Delta \mathbf{R}_j \rangle / (\langle \Delta \mathbf{R}_i \cdot \Delta \mathbf{R}_i \rangle \langle \Delta \mathbf{R}_j \cdot \Delta \mathbf{R}_j \rangle)^{1/2} \quad (5)$$

C_{ij} values vary in the range $-1 \leq C_{ij} \leq 1$. The upper and lower limits correspond to pairs of residues exhibiting fully correlated (same direction, same sense) and fully anticorrelated (same direction, opposite sense) motions, respectively. The particular case where $C_{ij} = 0$ refers to uncorrelated motions.

For simplicity, we concentrate on the structural elements listed in Table 2. These were determined above to play a key role in directing the most cooperative motions of the enzyme. Average correlations $\langle C_{ij} \rangle$ are calculated for each pair of structural elements, on the basis of all combinations of residues belonging to them. The resulting correlation map is presented in Figure 9. The two axes represent the serial indices of the individual structural elements. The elements in subunits α_1 and β_1 are assigned serial numbers 1–21, conforming with the first column of Table 2. The coenzyme bound to subunit β_1 is viewed as structural element 22. The latter is examined either as a PLP Schiff base (E) (1bks) or as an external aldimine E–Trp (2tys). The elements of subunits α_2 and β_2 are assigned numbers in the range of 23–44, in the same order as those defined for subunits α_1 and β_1 .

The contours in Figure 9 connect the pairs of structural elements subject to fixed correlation values. The most strongly correlated pairs ($C_{ij} \geq 0.8$) are enclosed by the green contours; these pairs undergo coherent, concerted movements in the same direction. The red contours, on the other hand,

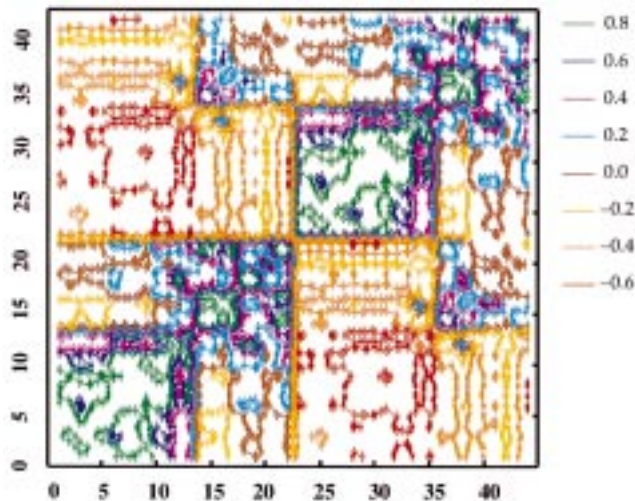


FIGURE 9: Correlation map for the orientational cross-correlations $\langle \Delta \mathbf{R}_i \cdot \Delta \mathbf{R}_j \rangle$ in the motions of residues, driven by the dominant modes of motion. Results are presented for 44 structural elements (9 in each α -subunit, 12 in each β -subunit, and 1 for each β -site substrate) showing distinctive dynamic features in the dominant modes of motion. See the first column of Table 2 for the definition of these structural elements. The axes refer to the serial number of the structural elements in Table 2, and the contours connect equally correlated regions, following the scale given on the right.

enclose the other extreme case of strongly anticorrelated ($C_{ij} \leq -0.6$) regions. The corresponding elements undergo concerted, but opposite direction, fluctuations in the global modes. For the intermediate regions, see the scale on the right of the map.

The following dominant features can be observed in the map. Elements within a given subunit are generally positively correlated. See the blocks along the diagonal. The α -subunit undergoes more coherent motions, indicated by the stronger orientational correlations between its individual elements, compared to those between the elements of the β -subunits. Subunits α_1 and α_2 are strongly anticorrelated. Subunits α_1 and β_2 (and similarly α_2 and β_1) exhibit anticorrelated motions, though not as pronounced as those between α_1 and α_2 . The behavior of the contiguous subunits is more complex, as will be elaborated next.

Figure 10 displays the cross-correlations between the β - β hinge residues and the other structural elements being investigated here. The curves represent horizontal (or vertical) strips of the correlation map (Figure 9), at three structural elements, with serial indices 14, 15', and 16 (i.e., β_1 -subunit residues 48-67, 77-89, and 337-346, respectively; see Table 2). The curve for the fourth β - β hinge site in the same subunit (element 17; β_1 -subunit residues 337-346) closely coincides with that of element 15'. The types of structural elements, across the strip(s) of the map, are indicated along the abscissa of Figure 10. The regions corresponding to subunits α_1 , β_1 , α_2 , and β_2 are separated by lightface dashed vertical lines. The arrows on the upper abscissa indicate the indices (22 and 44) of the β -site substrates.

The β - β hinge sites are strongly coupled to each other, as inferred from the maxima in Figure 10 at positions 14-17. More importantly, their motions are highly correlated with that of the substrate (element 22) in the same subunit. Correlations transmitted across the β - β interface are also distinguishable. These are evidenced by the peaks at the β - β

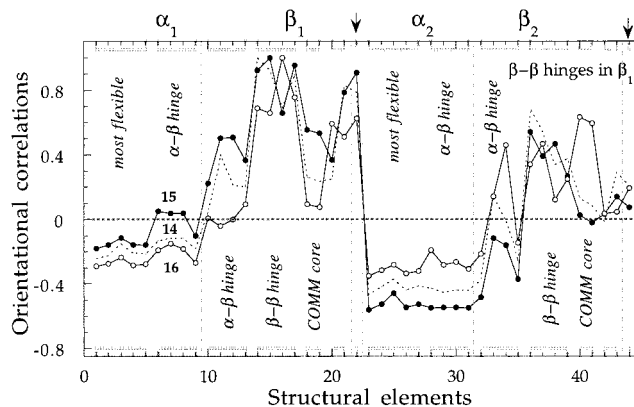


FIGURE 10: Orientational cross-correlations between the β - β hinge residues (elements 14-17; see the first column in Table 2) and all other structural elements distinguished by their distinctive behavior in the dominant modes of motion of the tetramer, and grouped according to their characteristic dynamics (see the last column in Table 2). The arrows on the upper abscissa indicate the positions of the β -subunit substrates (elements 22 and 44). The dashed vertical lines denote the separation between respective subunits α_1 , β_1 , α_2 , and β_2 , indicated by the labels along the upper abscissa.

hinge and COMM core regions of subunit β_2 . Overall, the β - β hinge residues appear to have a pivotal role, being anticorrelated with both α -subunits, strongly correlated with the substrate in the same subunit, and somewhat coupled to the hinge residues and COMM core in β_2 .

It is interesting to note that the COMM core residues in β_1 are correlated with β - β hinge residues β_1 337- β_1 346 in β_2 , while also moving coherently with α - β hinge residues β_1 174- β_1 179 in β_1 . See Figure 11a. Here, the abscissa refers again to the serial index of the structural elements listed in the first column of Table 2. Thus, the movements of the COMM core are being simultaneously modulated by the α - β hinge residues in the same subunit, and by the β - β hinge residues in the adjoining β -subunit. The existence of such intersubunit communication is consistent with the close interactions already observed in Figure 6b.

A direct examination of the orientational behavior of the β -site substrate, and its perturbation in the presence of formation of an external aldimine, E-Trp, yields the curves in Figure 11b. The solid curve therein depicts the behavior of the coenzyme PLP in wt structure 1bks. The regions showing the strongest orientational correlations with the PLP are β - β hinge sites β_1 77- β_1 89 and β_2 376- β_2 379. On the other hand, a strong anticorrelation with the entire subunit α_2 is observed. The dotted curve shows the changes in correlations observed in the mutant β_1 K87T α_2 β_2 , relative to the wt structure. The COMM core region and α - β hinge residues β_1 174- β_1 179 in the same subunit are observed here to be the most strongly affected regions. Apparently, a substantial increase in the extent of their orientational coupling to the substrate takes place in the presence of an external aldimine.

DISCUSSION

The changes in structure induced upon substrate binding, or upon intermediate formation in the different subunits, are now well established from X-ray crystallographic measurements. Here, we have searched for the accompanying changes to the dynamics of the tetrameric enzyme, which might

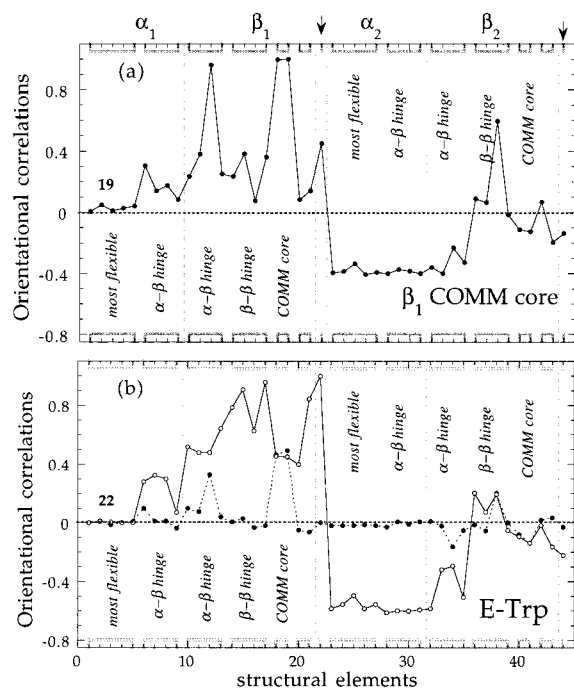


FIGURE 11: (a) Orientational cross-correlations between β_1 COMM core residues β_{155} – β_{170} (structural element 19 in Table 2) and the other structural elements. The peaks at positions 12 and 36 denote the respective strong correlations of the β_1 COMM core residues with α – β hinge residues β_{174} – β_{179} in subunit β_1 and with β – β hinge residues β_{337} – β_{346} in β_2 . (b) Same as panel a for correlations with the substrate bound to the β_1 -reaction site. The dashed line represents the changes in orientational correlations observed in 2tys, relative to those of the wt structure (1bks). The most strongly affected regions therein are the β_1 COMM core (18 and 19) and β_1 α – β hinge residues β_{174} – β_{179} .

explain the allosteric effects transmitted across the subunits over distance ranges of 20–30 Å.

Toward this aim, first the global dynamic characteristics intrinsic to the particular molecular architecture of TRPS complexes were investigated. Second, the changes brought about by the presence of different substrates were examined. Several questions were addressed. A crucial one was whether the formation of an external aldimine, E–Ser or E–Trp, with PLP in the β -subunit, induces long-range changes in correlated motions, and if so which structural elements play a key role in coordinating the conformational switches.

Overview of Global Dynamics. The dynamic preferences of TRPS complexes on a global scale were determined by focusing on the first principal mode of motion. Little qualitative difference was observed between the principal mode shape of the different structures, as illustrated in Figure 3. This mode shape is interpreted as the generic behavior of the enzyme itself in the tetrameric form, given its particular three-dimensional architecture.

Our analysis of the principal mode shape revealed three distinct categories of residues (Table 2): (i) residues enjoying a high conformational flexibility, mostly located at solvent-exposed regions of the α -subunits, (ii) constrained residues acting as hinges for the relative motions of the α - and β -subunits, mostly located at the α – β interface, and (iii) constrained residues acting as hinges for the relative motion of the two β -subunits, and for the relative motion of the two domains of the β -subunits, positioned near the β – β inter-subunit interface. These were shown in green, red (or pink),

and magenta, respectively, in Figures 4 and 6a. On the basis of the common trend observed for dynamics–function relationships in other biomolecular systems, we tentatively associate these mechanical properties with the following functions. The first group may be involved in substrate recognition, here for the α -reaction reactants. The second modulates the binding and catalytic activity at a nearby active site, here the α -site. Additionally, this group presently assumes an important role in the concomitant communication between the two subunits, as suggested by its extension toward the β – β interface via α -helix β H1 (Figure 6). Finally, the third group (red and magenta regions in the β – β dimer shown in Figure 6b) is involved in the β -reaction catalysis, in the transmission of cooperative conformational motions across the β – β interface, and in modulating the opening and closing of the substrate channeling tunnel between the N- and C-terminal domains of the β -subunits. The latter mechanism of motion is ensured by the β – β hinge residues colored magenta in Figure 6b. We now consider these results in further detail.

Potential Sites of Substrate Recognition in the α -Subunit.

The C-terminal portion of α -subunits beyond loop α L6 was distinguished by high amplitude motions, persisting under the action of a dominant set of modes (Table 2). A five-residue stretch in loop α L6 (α_{179} – α_{183}) assumes a hinge-bending role in providing the flexibility of the C-terminal portion (α_{192} – α_{268}), or particularly those for helices α H6 and α H8. Likewise, α – β hinge residues α_{54} – α_{60} in loop α L2 appear to mediate the mobility of N-terminal helix α H1. These helices preserve their flexibility under the joint effect of the larger subset of dominant modes (Figure 5a).

Such highly flexible regions have been observed in our previous GNM analyses for other proteins, or complexes, to coincide with substrate recognition sites (25–28, 31); it remains to be seen if the peak residues on α H8 and α H1 and at the N-terminus of α H6, along with those in α H5 and α H2 in the presence of β -site substrates, are likewise involved in IGP or IPL recognition. Loop α L6 was shown to be stabilized, together with loop α L2, upon substrate binding (7), which may be consistent with the fact that no further drive for recognition is required following substrate binding.

Unfolding Kinetics. Previous comparisons of theoretical ms fluctuations of individual residues in a series of proteins with corresponding H–D exchange protection factors under native or mildly denaturing conditions indicated that residues subject to relatively high-amplitude motions in the folded state are more likely to unfold first (24). In TRPS complexes, the C-terminal portions (α_{192} – α_{268}) of α -subunits are found to have an enhanced flexibility compared to the remainder of the α -subunit. Interestingly, GdnHCl-induced unfolding studies with the α -subunit and with its two proteolytic fragments have provided evidence for a stepwise unfolding of the two domains (18, 32); the C-terminal domain becomes disordered at low GdnHCl concentrations, while the N-terminus remains folded. This behavior has been confirmed in many kinetic studies [see Matthews and collaborators (33–35)]. Thus, the α -subunit of the TRPS $\alpha_2\beta_2$ complex provides another example in which early unfolding is correlated with high flexibility.

Critical Loci at the α – β Interface. Four stretches of residues are proposed here in each subunit to form the hinge-

bending sites for the relative motion of the α - and β -subunits (see Table 2). The involvement of hinge-bending sites in binding at the active site and catalysis is a common feature observed in other proteins, such as HIV-1 protease (25) and HIV-1 reverse transcriptase (27). We will now consider the α - β hinge sites identified in TRPS. Results obtained for the α - and β -subunits will be separately discussed next, along with a description of their couplings and role in allosteric communication.

Hinge Sites in α -Subunits. The most pronounced critical loci of α -subunits are those in loops α L2 and α L6. These are proposed to control the α - β hinge bending motions, and also modulate the α -reaction. The involvement of α L2, and in particular that of α Asp60 in α L2, in the α -reaction catalysis, and in allosteric communication, has now been well-established by several experiments (9, 16, 36). Likewise, loop α L6 is important for ligand binding and communication between the α - and β -subunits. The latter is indicated by the insensitivity of the "nicked" $\alpha_2\beta_2$ complex to inhibitors after the proteolytic cleavage of α L6 at α Arg188 (37). The same loop, following strand α S6, is also shown in TIM barrels to undergo a change from an "open" to a "closed" state upon substrate binding (38–40). Residue α Thr183 in α L6 is ascribed a concomitant role in catalytic activity, on the basis of its interaction with the catalytically active residue α Asp60, and the fact that its substitution results in complete inactivity toward IGP (5, 7). The lower substrate binding affinity observed (11) in the mutant α R179L is likewise consistent with the role ascribed to residues α 179– α 183 for binding substrates at the α -reaction site.

The hinge site center around Gly181 in α L6 is determined here from PDB file 1trs. This is the only currently available structure in which residues participating in loop α L6 are partly visible. This feature was attributed to the presence of substrates bound on both subunits (5). The obstruction in conformational mobility of α L6 upon binding of ligands was also indicated by the prevention of tryptic cleavage (41). The restriction in conformational mobility is consistent with the hinge role of residues α 179– α 183 presently determined.

GNM analysis yields two additional hinge sites in the α -subunit near the α - β interface: α 102– α 110 and α 129– α 136. No experimental data supporting the critical role of these residues are presently available, to our knowledge, apart from the observation that the substitution of the conserved proline, α Pro132, with glycine greatly weakens the association of the α - and β -subunits (42). However, our calculations suggest that these residues also participate in the cooperative motions at the α - β interface. These regions are engaged in close interactions with the β -subunit α - β hinge residues, like the couplings between α L6 and β H6 (see below). Closely interacting pairs include amino–aromatic or aromatic–aromatic pairs such as α Asn108– β Gly292, α Phe107– β Tyr16, α Asp130– β Pro18, α Pro132– β Gln19, and α Glu135– β Tyr16.

α - β Hinge Sites in β -Subunits. Among the β -subunit hinge-bending sites presently identified and suggested to play a key role in processing movements relevant to catalytic activity, we first notice β 174– β 179 in β -subunit helix β H6, and β 277– β 283 in the central part of the long loop connecting β S8 and β H10. See Figure 6b.

Let us first consider β H6 residues β 174– β 179. These interact simultaneously with (i) α -subunit hinge residues α 179– α 183 on helix α L6 and (ii) β -subunit α - β hinge

residues β 18– β 44. Both of the sites (i and ii) are in turn closely coupled to loop α L2 containing the α -reaction site. The coupling between α L2, α L6, and β H6 is supportive of the mechanism proposed (7) for communicating substrate binding from the α - to the β -site: mutual stabilization of α L2 and α L6, complemented by interactions between α L2 and β H6 to establish the intersubunit connection. Our analysis of cross-correlations discloses, in fact, the important role of β H6 residues β 174– β 179 in transmitting the change in the dynamics of the COMM core region to the α - β interface, and thereby to the α -reaction site.

The dynamics of residues β 277– β 283, on the other hand, is coupled to that of residues β 174– β 179, provided that an external aldimine is present in the β -site. It is interesting to note that residues β 277– β 283 precisely include the two aromatic residues, β Phe280 and β Tyr279, which act as a molecular gate for opening and closing the hydrophobic tunnel to allow or obstruct the passage of substrate (4, 5, 16, 43, 44) (see Figure 4), and another residue, β Gly281, whose mutation (G281R) was found to inactivate the TRPS from *Escherichia coli* and was attributed to the prevention of a conformational change that affects catalytic properties and subunit interaction (45). In particular, β Tyr279 emerges here as a critical locus for the global motion of the enzyme (Table 2).

Two more regions are distinguished by very sharp peaks in Figure 3b: β 14– β 24 and β 288– β 295. The stretch of residues β 288– β 295 moves concertedly with β 277– β 283 as shown by their cross-correlations, whereas the region of residues β 14– β 24, extended in the enlarged set of dominant modes to cover β H1 and β H2 residues β 18– β 44, plays a dominant role in transmitting the hinge-bending movements of the α - β interface across the overall tetramer, as will be further discussed below.

Critical Loci at the β - β Interface. Like the hinge-bending sites identified at the α - β interface, those near the β -site are implied by the GNM to play a key role in binding of substrate, and in providing the mechanical framework for catalytic function. In view of their close proximity in space to the active site of the β -subunit, it is conceivable that these are involved in regulating the β -reaction. Their direct involvement in the β -reaction became clear, in fact, from the analysis of the orientational cross-correlations driven by the dominant modes of motions.

In all five structures that have been examined, the most severely constrained region of the tetramer under the action of the dominant 10 modes emerged as the stretch of residues β 77– β 89. This region is of interest for two reasons. First, it includes residue β Lys87 to which the PLP is covalently linked, and second, it is positioned at the connection between the N- and C-terminal domains of the β -subunit. See Figure 8. The lowest minima in the fluctuation distributions calculated for the five TRPS complexes (Figure 3) were all found to be at Leu80, succeeded by Gly84, His82, Leu81, and Gly83. Thus, the sequence LLHGG (residues 80–84) is distinguished in this study by its critical role as an anchor, near the β -reaction site. The region of residues β 77– β 89 is apparently complemented by residues β 48– β 67, β 204– β 206, and β 376– β 379, in processing the motions related to indole channeling between the α - and β -sites. These residues are indeed located at the links between the two domains of the β -subunit. They are involved in regulating the mutual movements of the two domains that directly enlarge or

subdomains, etc. The presently identified α - β and β - β hinge sites indeed conform to these requirements. They enclose the active site; they are located on an intersubunit (α - β or β - β) interface or at an interdomain connection. Most of them are located on loops, except for a few helical sites which possibly act as molecular shafts permitting rotational motions about their axes. These observations suggest that catalytic sites are designed to be at regions constrained in the global motion, being at the same time near interfaces between subunits, or clefts between domains.

Another important implication relates to residue conservation. Mutations at the presently identified hinge sites are likely to be consequential for disrupting the cooperativity underlying the overall multifunctional catalytic activity of the enzyme. We note that the COMM core residues, while participating in the transmission of conformational motions, could be tolerant to mutations, because they enjoy sufficient flexibility. However, the sites subject to the most severe constraints in the global mode, such as the α - β and/or β - β hinge sites, would be expected to be conserved from a functional point of view. The stretch of residues LLHGG at β 80- β 84 emerged here, in particular, as the most severely constrained region of the tetramer. The fact that this region is highly conserved is supportive of the expected relationship between the critical role in the global mode and residue conservation for functionally related processes.

ACKNOWLEDGMENT

We are grateful to Dr. Edith Miles for many insightful suggestions and valuable comments during the course of this work, and for her careful reading of the manuscript. Also, we are grateful to Dr. Sangkee Rhee for useful remarks and to Dr. Craig Hyde for providing the coordinates of the refined wt structure prior to publication.

REFERENCES

- Ahmed, S. A., Miles, E. W., and Davies, D. R. (1985) *J. Biol. Chem.* 260, 3716-3718.
- Hyde, C. C., Ahmed, S. A., Padlan, E. A., Miles, E. W., and Davies, D. R. (1988) *J. Biol. Chem.* 263, 17857-17871.
- Hyde, C. C., and Miles, E. W. (1990) *Biotechnology* 8, 27-32.
- Rhee, S., Parris, K. D., Ahmed, S. A., Miles, E. W., and Davies, D. R. (1996) *Biochemistry* 35, 4211-4221.
- Rhee, S., Parris, K. D., Hyde, C. C., Ahmed, S. A., Miles, E. W., and Davies, D. R. (1997) *Biochemistry* 36, 7664-7680.
- Rhee, S., Miles, E. W., and Davies, D. (1998) *J. Biol. Chem.* 273, 8553-8555.
- Schneider, T. R., Gerhardt, E., Liang, P.-H., Anderson, K. S., and Schlichting, I. (1998) *Biochemistry* 37, 5394-5406.
- Kawasaki, H., Bauerle, R., Zon, G., Ahmed, S. A., and Miles, E. W. (1987) *J. Biol. Chem.* 262, 10678-10683.
- Nagata, S., Hyde, C. C., and Miles, E. W. (1989) *J. Biol. Chem.* 265, 7987-7993.
- Brzovic, P. S., Kayastha, A. M., Miles, E. W., and Dunn, M. F. (1992) *Biochemistry* 31, 1180-1190.
- Brzovic, P. S., Haig, C. C., Miles, E. W., and Dunn, M. F. (1993) *Biochemistry* 32, 10404-10413.
- Rowlett, R., Yang, L., Ahmed, S. A., McPhie, P., Jhee, K., and Miles, E. W. (1998) *Biochemistry* 37, 2961-2968.
- Dunn, M. F., Aguilar, V., Brzovic, P. S., Drewe, W. F. J., Houben, K. F., Leja, C. A., and Roy, M. (1990) *Biochemistry* 29, 8598-8607.
- Anderson, K. S., Miles, E. W., and Johnson, K. A. (1991) *J. Biol. Chem.* 266, 8020-8033.
- Lane, A. N., and Kirschner, K. (1991) *Biochemistry* 30, 479-484.
- Brzovic, P. S., Sawa, Y., Hyde, C. C., Miles, E. W., and Dunn, M. F. (1992) *J. Biol. Chem.* 267, 13028-13038.
- Peracchi, A., Bettati, S., Mozzarelli, A., Rossi, G. L., Miles, E. W., and Dunn, M. F. (1996) *Biochemistry* 35, 1872-1879.
- Miles, E. W. (1991) The Tryptophan Synthase $\alpha_2\beta_2$ Multi-enzyme Complex: Relationship of the Amino Acid Sequence and Folding Domains to the Three-dimensional Structure, in *Conformations and Forces in Protein Folding* (Nall, B. T., and Dill, K. A., Eds.) pp 115-124, American Association for the Advancement of Science, Waldorf, MD.
- Miles, E. W., Ahmed, S. A., Hyde, C. C., Kayastha, A. M., Yang, X., Ruvinov, S. B., and Lu, Z. (1994) in *Molecular Aspects of Enzyme Catalysis* (Fukui, T., and Soda, K., Eds.) pp 127-146, Kodansha Ltd., Tokyo, Japan.
- Miles, E. W. (1995) Tryptophan Synthase: Structure, Function, and Protein Engineering, in *Subcellular Biochemistry: Proteins: Structure, Function, and Protein Engineering* (Biswas, B. B., and Roy, S., Eds.) pp 207-254, Plenum Press, New York.
- Pan, P., Woehl, E., and Dunn, M. F. (1997) *Trends Biochem. Sci.* 22, 22-27.
- Bahar, I., Atilgan, A. R., and Erman, B. (1997) *Folding Des.* 2, 173-181.
- Haliloglu, T., Bahar, I., and Erman, B. (1997) *Phys. Rev. Lett.* 79, 3090-3093.
- Bahar, I., Wallqvist, A., Covell, D. G., and Jernigan, R. L. (1998) *Biochemistry* 37, 1067-1075.
- Bahar, I., Atilgan, A. R., Demirel, M. C., and Erman, B. (1998) *Phys. Rev. Lett.* 80, 2733-2736.
- Bahar, I., and Jernigan, R. L. (1998) *J. Mol. Biol.* 281, 871-884.
- Bahar, I., Erman, B., Jernigan, R. L., Atilgan, A. R., and Covell, D. G. (1998) *J. Mol. Biol.* 285, 1023-1037.
- Demirel, M. C., Atilgan, A. R., Jernigan, R. L., Erman, B., and Bahar, I. (1998) *Protein Sci.* 7, 2522-2532.
- Flory, P. J. (1976) *Proc. R. Soc. London, Ser. A* 351, 351-380.
- Tirion, M. M. (1996) *Phys. Rev. Lett.* 77, 1905-1908.
- Lustig, B. R., Bahar, I., and Jernigan, R. L. (1998) *Nucleic Acids Res.* 26, 5212-5217.
- Miles, E. W., Yutani, K., and Ogasahara, K. (1982) *Biochemistry* 21, 2586-2592.
- Beasty, A. M., Hurle, M. R., Manz, J. T., Stackhouse, T., Onuffer, J. J., and Matthews, C. R. (1986) *Biochemistry* 25, 2965-2974.
- Stackhouse, T. M., Onuffer, J. J., Matthews, C. R., Ahmed, S. A., and Miles, E. W. (1988) *Biochemistry* 27, 824-832.
- Chrnyk, B. A., and Matthews, C. R. (1990) *Biochemistry* 29, 2149-2154.
- Rhee, S., Miles, E. W., Mozzarelli, A., and Davies, D. R. (1998) *Biochemistry* 37, 10653-10659.
- Miles, E. W. (1991) *J. Biol. Chem.* 266, 10715-10718.
- Lolis, E., Alber, T., Davenport, R. C., Rose, D., Hartman, F. C., and Petsko, G. A. (1990) *Biochemistry* 29, 6609-6618.
- Lolis, E., and Petsko, G. A. (1990) *Biochemistry* 29, 6619-6625.
- Wierenga, R. K., Noble, M. E. M., Postma, J. P. M., Groendijk, H., Kalk, K. H., Hol, W. G. J., and Opperdoes, F. R. (1991) *Proteins* 10, 33-49.
- Ruvinov, S. B., and Miles, E. W. (1992) *FEBS Lett.* 299, 197-200.
- Ogahasara, K., Hiraga, K., Ito, W., Miles, E. W., and Yutani, K. (1992) *J. Biol. Chem.* 267, 5222-5228.
- Stroud, R. M. (1994) *Nat. Struct. Biol.* 1, 131-134.
- Ruvinov, S. B., Yang, X. J., Parris, K. D., Banik, U., Ahmed, S. A., Miles, E. W., and Sackett, D. L. (1995) *J. Biol. Chem.* 270, 6357-6369.
- Zhao, G., and Somerville, R. I. (1992) *J. Biol. Chem.* 267, 526-541.
- Kishore, N., Tewari, Y. B., Akers, D. L., Goldberg, R. N., and Miles, E. W. (1998) *Biophys. Chem.* 73, 265-280.
- Pearson, D. S. (1977) *Macromolecules* 10, 696-701.